A.-C. Wong, J. R. Clark, and C. T.-C. Nguyen, "Anneal-activated, tunable, 65MHz micromechanical filters" *Digest of Technical Papers*, 10th International Conference on Solid-State Sensors and Actuators, Sendai, Japan, June 7-10, 1999, pp. 1390-1393.

# Anneal-Activated, Tunable, 68MHz Micromechanical Filters

*Ark-Chew Wong, John R. Clark and Clark T.-C. Nguyen*

Center for Integrated Microsystems
Department of Electrical Engineering and Computer Science
University of Michigan
Ann Arbor, Michigan 48109-2122

## ABSTRACT

Tunable, two-pole micromechanical (μmechanical) filters for communications applications, each comprised of a network of interconnected clamped-clamped and sliding-support μmechanical beams, are demonstrated with center frequencies from 50-68MHz and percent bandwidths less than 2%, all with insertion losses less than 9dB. The demonstrated 68MHz center frequency represents the highest frequency yet attained by a two-pole filter and was attained by a combination of dimensional scaling and the introduction of two key design features: (1) electrodes allowing *in situ* localized annealing of devices to enhance resonator *Q*'s, and thus, minimize filter loss; and (2) additional electrodes flanking the input and output allowing voltage-controlled tuning of each individual resonator frequency to correct for increased process variations in this scaled technology.

## I. INTRODUCTION

Micromechanical electronic bandpass filters with frequencies in the low-VHF range (e.g., 35MHz [1]) have recently been demonstrated with percent bandwidths less than 0.2% and associated insertion losses less than 2dB—numbers that rival (and even better in some cases) those of off-chip crystal and SAW filters used in present-day wireless transceivers. Given their compatibility with IC technologies, μmechanical filters can potentially serve as direct on-chip replacements for their bulky off-chip SAW and crystal counterparts, allowing substantial size and power reductions in wireless transceivers, perhaps even paving the way for single-chip implementations. In order for this to become a commercial reality, however, the frequency of μmechanical filters must be extended.

This work investigates frequency extension through direct dimensional scaling of capacitively-transduced, flexural-mode beam μmechanical filters, and in the process demonstrates filters with center frequencies up to 68MHz, percent bandwidths less than 2%, and associated insertion losses less than 9dB. In considering this "brute force" scaling approach to frequency extension, several physical phenomena that ultimately constrain filter performance characteristics are uncovered. This paper gives particular emphasis to such phenomena, which include structural topography, finite anchor elasticity, anchor dissipation, transducer nonidealities, and even contamination, which becomes increasingly important on this micro-scale. The paper concludes with design suggestions that eliminate the majority of the observed problems.

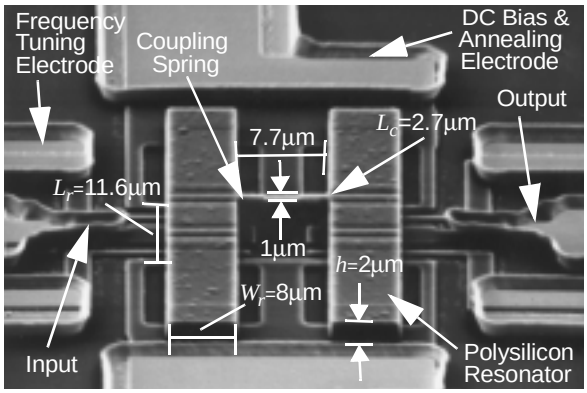


Fig. 1: SEM of a 68MHz μmechanical filter, equipped with $f_o$ tuning and anneal-activation electrodes.

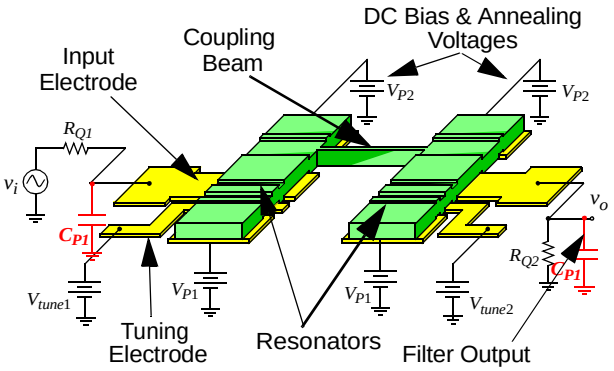


Fig. 2: Perspective-view schematic of the filter of Fig. 1 with electronics that enable passband correction and anneal-activation.

## II. STRUCTURE, OPERATION AND DESIGN OF VHF MICROMECHANICAL FILTERS

Figure 1 presents the scanning electron micrograph (SEM) of a 68MHz spring-coupled μmechanical filter with key components and dimensions identified. For enhanced clarity, Fig. 2 shows the perspective-view schematic for this filter in a bias and excitation scheme that enables passband correction and anneal-activation. As shown, this filter consists of two polycrystalline silicon μmechanical resonators, with identical geometries (and hence, identical resonance frequencies $f_o$), interlinked by a flexural-mode beam with stiffness $k_{s12}$ attached to each resonator at low-velocity locations [2]. Three electrodes underlie each resonator: one for input and output coupling, and two symmetrically placed for frequency tuning via voltage-controllable electrical stiffnesses [3]. In addition, electrodes to the anchors of each resonator are also

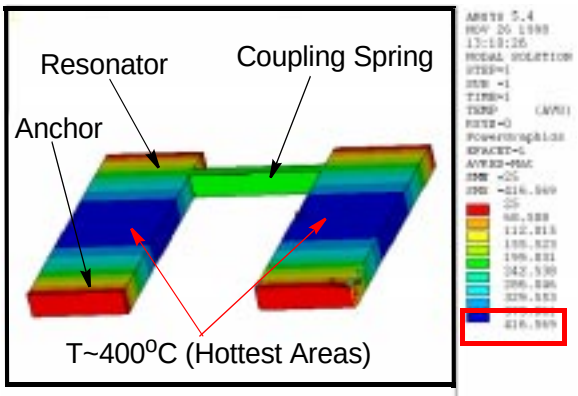


Fig. 3: Thermal profile of a localized annealed polysilicon micromechanical filter under $V_A$=1.5V, predicted via finite element analysis.

included to allow localized annealing [4] of the filter structure (via the current generated when $V_A=V_{P1}-V_{P2}$ is applied), which serves as a key anti-contamination measure used before (and sometimes during) filter operation under non-ideal test vacuum environments. Figure 3 presents the thermal topography over a 50MHz filter with $V_A$=1.5V as predicted by finite element simulation using ANSYS.

To operate this filter, the structure is biased to a dc voltage $V_P \sim (1/2)(V_{P1}+V_{P2})$, and an ac input signal $v_i$ is applied to the input electrode through termination resistor $R_{Q1}$. When the frequency of $v_i$ falls within the filter passband (set by the $f_o$ of the resonators and the $k_{s12}$ of the coupling beam), the whole structure is forced into vibration, at which point an output voltage is generated across output termination resistor $R_{Q2}$, then buffered to a network analyzer. In effect, electrical signals at the input are converted to mechanical signals, processed in the mechanical domain, then reconverted to electrical signals at the output, ready for further processing by subsequent electrical stages.

The center frequency of a μmechanical filter using identical resonators is equal to the frequency of those resonators and given by: [5]

$$f_o = \frac{1}{2\pi}\sqrt{\frac{k_r}{m_r}} = 1.03\kappa\sqrt{\frac{E}{\rho}}\frac{h}{L_r^2}\left(1-\left\langle\frac{k_e}{k_m}\right\rangle\right)^{1/2} \qquad (1)$$

where $k_r$ and $m_r$ are the dynamic stiffness and mass of the beam, respectively; $E$ and ρ are the Young's modulus and density of the structural material, respectively; $h$ and $L_r$ are geometric dimensions indicated in Fig. 1; κ is a scaling factor that models the effects of surface topography; and the function $\langle k_e/k_m \rangle$ models the effect of an electrical spring stiffness $k_e$ that arises when a bias voltage is applied across the electrode-to-resonator gap, and that subtracts from the mechanical stiffness [5]. Due to action of the $\langle k_e/k_m \rangle$ term, $f_o$ can be tuned by merely adjusting either $V_P$ or the voltages $V_{tune1}$ and $V_{tune2}$ in Fig. 2. For a 50MHz clamped-clamped beam μresonator a frequency excursion of 4.3% was measured over a 15V range in tuning voltage. The degree of tuning is also a function of beam frequency (actually, of stiffness $k_r$) and electrode-to-resonator gap spacing $d$ [5].

From (1), assuming that the thickness dimension $h$ is fixed by technological considerations, frequency increases are most conveniently achieved by shortening the beam length $L_r$. As $L_r$ is shortened, the electrode-to-resonator gap $d$ must also be scaled so that the filter termination resistance $R_{Qn}$ remains the same. ($R_{Qn}$ often must take on very specific values from 50-2,000Ω in order to properly impedance match to adjacent electronic stages in transceiver applications.) More specifically, the value of $R_{Qn}$ required by a filter using a particular resonator design is given by [2]:

$$R_{Qn} \approx \frac{P_{BW}}{q_n \omega_o}\frac{k_r}{\varepsilon_o A_o}\frac{d^4}{V_P^2} \qquad (2)$$

where $P_{BW}$ is the filter percent bandwidth, $q_n$ is a normalized $q$ parameter obtained from a filter cookbook [6], $\varepsilon_o$ is the permittivity in vacuum, and $A_o$ is the electrode-to-resonator overlap area. Given that shortening $L_r$ entails a large stiffness $k_r$ increase, with a relatively small change in mass $m_r$, and assuming that $V_P$ is fixed by supply voltage considerations, (2) requires that $d$ shrink to maintain the value of $R_{Qn}$. Thus, a $d$ <400Å is often required for filters with $f_o$'s from 50-100MHz.

## III. FABRICATION

Micromechanical filters with frequencies exceeding 50MHz were fabricated using a polysilicon surface micromachining process similar to those used to construct previous low-VHF range filters [1,2], except for the use of even smaller gap spacings on the order of 300Å. Although a seemingly minor change from previous processes, the need for such small gaps actually substantially complicates the release procedure for VHF devices.

In particular, because diffusion is difficult through small gaps for both reactants and etch by-products [7], release etch times are much longer than for previous large-gapped surface micromachining processes (e.g., 20 min. for 300Å gaps in 48.8 wt. % HF, as opposed to ~2 min. for 2μm gaps). Due to a finite rate of attack by hydrofluoric acid (HF) on heavily-doped polysilicon, longer release etch times often result in corrosion of interconnect, with consequent resistivity increases, or even removal of interconnect entirely. Furthermore, and perhaps more importantly, etch by-product residues that remain in the gap after release behave as physical dampers and can severely degrade the $Q$ of a given device. In severe cases (e.g., solid residues), resonator vibration might even be prevented entirely.

In an attempt to circumvent the above, the hydrocarbon-based surfactant, Triton X, was incorporated into some of the HF release etch solutions to both suppress the build-up of etch by-products and reduce the adhesion of particulates on the beam surfaces. In addition, the release step was followed by extensive cleaning procedures, involving repeated rinses in piranha and DI water, and sometimes even an additional supercritical $CO_2$ cleaning step. The latter was not needed to prevent stiction of devices (since the high stiffness

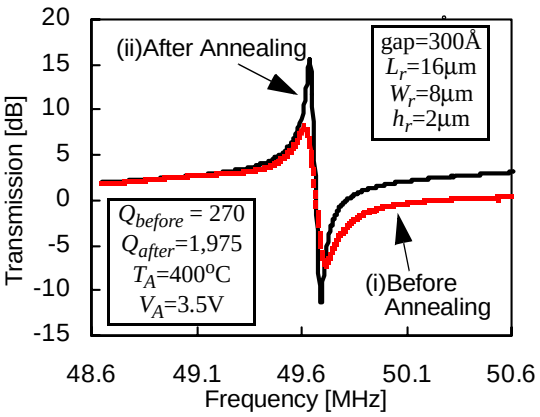


Fig. 4: Measured frequency characteristics for a 50MHz micromechanical resonator (i) before and (ii) after *in situ* localized anneal-activation.

of VHF devices prevents sticking), but rather to clean devices and purge contaminants from gaps.

## IV. EXPERIMENTAL RESULTS

A custom-built vacuum chamber was utilized for testing. This chamber provided low pressures down to 50µTorr (via turbo-molecular pumping) and was capable of housing both the chip under test and buffering electronics in close proximity on a common pc board inserted within the chamber. The ability to place devices and electronics in close proximity allowed substantial reduction of interconnect parasitics and proved essential in measuring VHF resonators.

Unfortunately, at least in these early runs, the additional steps taken to insure unclogged electrode-to-resonator gaps and to insure the cleanliness of device surfaces were not 100% effective. In particular, without the use of surfactant-enriched HF in the release process, only about 25% of the filters on any given die were operable immediately after fabrication. The rest could not be operated without an additional post-fabrication localized annealing step immediately before operation. In effect, the majority of filters required "anneal-activation" for proper functionality. The use of surfactant-enriched HF in the release process increased the number of devices operable without annealing to about 75%.

To illustrate the utility of anneal-activation in our vacuum test set-up, Fig. 4 presents measured frequency characteristics for a 50MHz, 300Å-gapped µresonator before and after *in situ* localized annealing, respectively, clearly showing a $Q$ increase from 270 to 1,975 upon application of $V_A$=1.5V (to achieve ~400°C while testing). The $f_o$ increase observed upon annealing suggests a contaminant removal mechanism for $Q$ enhancement. Such a mechanism is further supported by the fact that only resonators with electrode-to-resonator gaps less than 500Å require anneal-activation, suggesting that losses are amplified when contamination finds its way into a tiny gap. Again, not all small-gapped resonators required annealing to attain high $Q$; only 75% of them, and those that did not were visibly cleaner devices.

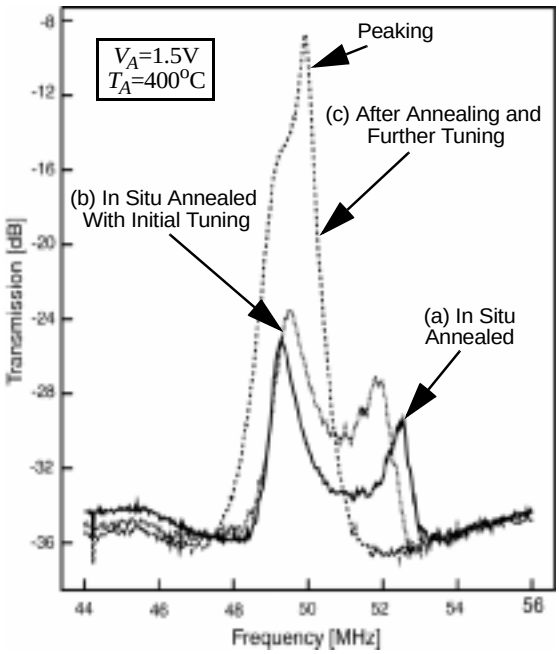


Fig. 5: Measured frequency characteristics for a 50MHz µmechanical filter obtained (a) upon *in situ* annealing; (b), (c) after tuning the $f_o$'s of individual resonators via $V_{tune}$ voltages.

Anneal-activation is exploited further in Fig. 5, which summarizes the procedure required to attain a properly functioning filter immediately after fabrication and in our turbo-pumped vacuum test set-up. At first, without any annealing, a frequency response measurement yields nothing in the expected range of the filter; i.e., only noise is observed. With the introduction of *in situ* localized annealing, the mode peaks rise and become sharper (curve (a)), indicating an increase in $Q$. Annealing is then stopped, and tuning voltages $V_{tune,i}$ are adjusted to move the mode peaks to their proper locations, resulting finally in the desired spectrum of curve (c), where an insertion loss of 8dB for a 2% bandwidth centered at 50MHz is seen. Figure 6 presents similar data for a 68MHz filter.

Some qualitative data gauging the susceptibility of µmechanical filters to real-time contamination was also inadvertently obtained by virtue of our test chamber. In particular, although instrumental in the measurement of VHF spectra, the pc-board within the chamber also proved to be an uninvited source of contaminants, providing a constant flow of outgassed contaminants over the chip under test. As a consequence, within this test chamber, a given filter functions properly for only about 30 minutes. After this time period, the filter insertion loss is observed to increase, indicating some amount of real-time $Q$-degradation in the resonators making up the filter, most likely caused by surface contamination or even trapping of contaminants with the electrode-to-resonator gap to produce a physical damper. A short 300s, 200°C activation-anneal at this point restores device operation for another 30 minutes.

The above data all support a contaminant based

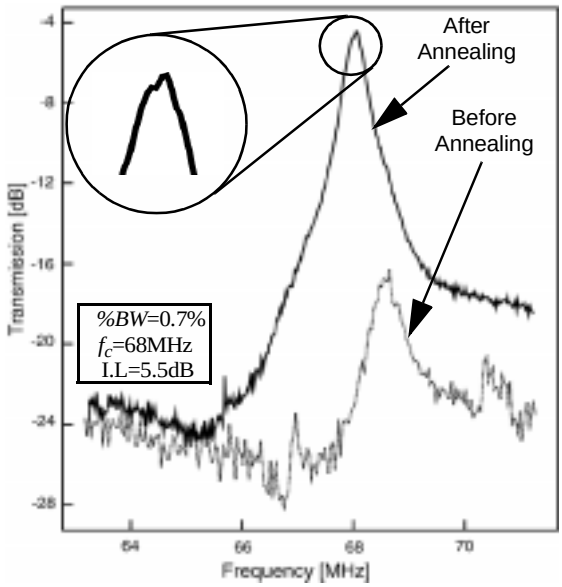


Fig. 6: Measured frequency characteristics for a 68MHz micromechanical filter (i) before and (ii) after *in situ* localized anneal-activation.

mechanism for *Q*-limiting in small-gapped, VHF range μmechanical resonators and filters. In particular, the fact that devices with gaps larger than 500Å can be operated without the need for annealing provides support for a mechanism where gap residues dominate the *Q* of resonators before annealing. In such a model, localized annealing then raises the temperature of the device, melting or evaporating away gap contaminants, thus allowing proper high-*Q* operation. However, gap residues do not seem to be solely responsible for *Q*-degradation, as even the *Q*'s of resonators with gaps larger than 500Å can still benefit from localized annealing. Thus, both surface and gap contamination seem to be working together (and perhaps with other internal loss mechanisms, e.g., hysteretic defects) to degrade the *Q*'s of VHF μmechanical resonators.

It should be noted, again, that not all filters required anneal-activation to function properly; only about 75% of them. The fact that not all filters require annealing to operate correctly, combined with evidence for a contamination removal mechanism for *Q*-enhancement, suggest that anneal-activation can be avoided altogether if a cleaner operation environment can be provided (perhaps via wafer-level encapsulation [8]) and if methods for removing gap residues can be further improved.

*Anchor Losses.*

Once contaminant losses are annealed away, other dissipation mechanisms begin to dictate resonator *Q*'s. For the case of VHF filters utilizing clamped-clamped beam resonators, anchor loss seems to be the next most important mechanism. Evidence for significant anchor loss mechanisms for VHF clamped-clamped beam resonators has already been reported in [9], where *Q*'s were seen to drop from 8,000 to only 300 for 8.5MHz and 70MHz μresonators, respectively.

The filter frequency characteristic in Fig. 5 provides even more compelling evidence that anchor losses are at work. In particular, this characteristic shows peaking on the right side of the passband, indicating that the anti-symmetric mode peak in the filter dynamic response exhibits a higher *Q* than the symmetric mode. This makes logical sense when one considers that in the (lower frequency) symmetric mode, the constituent resonators move in unison, both exerting forces on their anchors that then radiate energy into the substrate, lowering the *Q* of this mode. In the anti-symmetric mode, on the other hand, resonators vibrate with opposite phases, generating oppositely phased forces on their respective anchors, allowing partial cancellation of anchor forces, and resulting in less radiation into the substrate. Thus, the *Q* is higher for the anti-symmetric mode than for the symmetric mode, which is seen under measurement as a higher, sharper peak on the right side of the filter passband.

Needless to say, the peaking shown in Fig .5 (and Fig. 6) is not desirable. Thus, future VHF range filters should use resonators with better substrate isolation, such as balanced tuning forks or virtually levitated free-free beam designs [9].

## V. CONCLUSIONS

Two-pole VHF micromechanical filters utilizing clamped-clamped beam resonators have been demonstrated with good insertion loss and passband rejection. However, these resonators begin to exhibit deficiencies at mid-VHF frequencies, perhaps making them unsuitable for extension beyond VHF. Specifically, a requirement for small electrode-to-resonator gaps not only complicates the fabrication process, but can also compromise insertion loss performance in filters by increasing interconnect resistivity and enhancing susceptibility to contamination. Although localized annealing has been demonstrated as an effective measure against contamination-based loss mechanisms, such phenomena are perhaps best suppressed by improved release cleaning procedures and device encapsulation. As a further complication, the use of unbalanced clamped-clamped beams at VHF frequencies leads to excessive anchor losses that distort the passbands of the filters. Alternative resonator designs that reduce anchor losses, such as virtually levitated free-free beams [9], are expected to be more suitable for higher frequencies.

***Acknowledgment:*** This work was supported under grants from DARPA and NSF.

**References:**

[1] C. T.-C. Nguyen, *et al.*, *ISSCC*'99, pp. 78-79.
[2] F. D. Bannon III, *et al.*, *IEDM'96*, pp. 773-776.
[3] H. Nathanson, *et al*, *IEEE Trans. Electron Devices*, vol. ED-14, No. 3, pp. 117-133, March 1967
[4] K. Wang, *et al.*, *Tranducers'97*, pp.109-112.
[5] A.-C. Wong, *et al.*, *IEDM'98*, pp. 471-474.
[6] A. I. Zverev, *Handbook of Filter Synthesis.* New York: John Wiley & Sons, 1967.
[7] D. J. Monk, *et al.*, *Transducers'91*, pp. 647-650.
[8] K. S. Lebouitz, *et al.*, *MEMS'99*, pp. 470-475.
[9] K. Wang, *et al.*, *MEMS'99*, pp. 453-458, 1999